

Snake orbits and related magnetic edge states

J. Reijniers and F. M. Peeters*

*Departement Natuurkunde, Universiteit Antwerpen (UIA),
Universiteitsplein 1, B-2610 Antwerpen, Belgium*

(October 26, 2018)

We study the electron motion near magnetic field steps at which the strength and/or sign of the magnetic field changes. The energy spectrum for such systems is found and the electron states (bound and scattered) are compared with their corresponding classical paths. Several classical properties as the velocity parallel to the edge, the oscillation frequency perpendicular to the edge and the extent of the states are compared with their quantum mechanical counterpart. A class of magnetic edge states is found which do not have a classical counterpart.

73.40-c; 73.50-k; 73.23

I. INTRODUCTION

The transport properties of a two-dimensional electron gas (2DEG) subjected to a nonhomogeneous perpendicular magnetic field (periodically modulated or not) have been the focus of a great deal of research in recent years.¹ Current fabrication technologies permit to create nonhomogeneous magnetic fields on a nanometer scale by deliberately shaping or curving the 2DEG,² or by integration of superconducting^{3,4} or ferromagnetic materials^{5,6} on top of the 2DEG. This will add a new functional dimension to the present semiconductor technology and will open avenues for new physics and possible applications.⁷

Theoretically, the effect of nonhomogeneous magnetic fields on a 2DEG have been studied both in the ballistic and the diffusive regime. The resulting perpendicular magnetic field can act as a scattering centre,^{5,6,8} but can also bind electrons,⁹⁻¹² and so influence the transport properties of the 2DEG. In transport calculations one needs the electron states, which are obtained by solving the Schrödinger equation.

Müller¹³ studied theoretically the single particle electron states of a 2DEG in a wide quantum waveguide under the application of a nonuniform magnetic field and showed that in the case of a magnetic field modulation in one direction, transport properties also become one dimensional and electron states propagate perpendicularly to the field gradient.

Making use of this decoupling, the electron states for different nonhomogeneous magnetic field profiles along one dimension were investigated, i.e. for a periodically modulated magnetic field¹⁴⁻¹⁶, for magnetic quantum steps, barriers and wells in an infinite 2DEG^{17,18} and in a narrow waveguide.¹⁹

In this paper we consider an infinite 2DEG subjected to a step-like magnetic field, i.e abruptly changing in magnitude or polarity at $x = 0$, in one dimension (taken to be the x -direction). Preliminary results were presented in Ref. 20. First the situation for two opposite homogeneous magnetic fields with the same strength will be considered. The classical trajectories correspond to *snake orbits* and were already used in the seventies²¹ to describe electron propagation parallel to the boundary between two magnetic domains. Back then, one was interested in understanding the electron transport through multi-domain ferromagnets and it turned out to be more convenient to work with the classical trajectories than with the corresponding electron states, which allows one to use a semi-classical theory which reduces the complexity of the theory considerably. We are interested in transport through a 2DEG situated in a semiconductor in which the Fermi energy is orders of magnitude smaller than in the metallic systems of Ref. 21.

We will study thoroughly the quantum mechanics of such electron states in a 2DEG subjected to this step magnetic field profile, and we will compare them with their classical counterpart. We will discuss the energy spectrum and the corresponding electron states, and derive several properties. We will show the existence of states which have a velocity opposite to the expected classical orbits. Additionally, we will show that adding a background magnetic field modifies the spectrum and the states considerably.

The paper is organized as follows. In Sec. II we present our theoretical approach. In Sec. III we calculate the energy spectrum, the wavefunctions and their corresponding group velocity, and compare this with their quantum mechanical counterpart. In Sec. IV we study the influence of a background magnetic field on the quantum mechanical and classical behaviour. In Sec. V we focus on the negative velocity state, and finally, in Sec. VI, we construct time dependent states, and interpret them classically for several magnetic field profiles.

II. THEORETICAL APPROACH

We consider a system of noninteracting electrons moving in the xy -plane in the absence of any electric potentials. The electrons are subjected to a magnetic field profile $\vec{B} = (0, 0, B_z(x))$. First, we will study the electronic states near the edge of two magnetic fields with opposite strength

$$B_z(x) = B_0 [2\theta(x) - 1], \quad (1)$$

which is independent of the y -coordinate. Next, we will consider the influence of a background magnetic field B on these states, which results in the magnetic field profile

$$B_z(x) = B_0 [2\theta(x) - 1] + B. \quad (2)$$

In the following we will use $B^l = B_z(x < 0)$ and $B^r = B_z(x > 0)$, to denote respectively the magnetic field on the left and the right hand side of the magnetic edge.

The one-particle states in such a 2DEG are described by the Hamiltonian

$$H = \frac{1}{2m_e} p_x^2 + \frac{1}{2m_e} \left[p_y - \frac{e}{c} A(x) \right]^2. \quad (3)$$

Taking the vector potential in the Landau gauge,

$$\vec{A} = (0, xB_z(x), 0), \quad (4)$$

we arrive at the following 2D Schrödinger equation

$$\left\{ \frac{\partial^2}{\partial x^2} + \left[\frac{\partial}{\partial y} + ixB_z(x) \right]^2 + 2E \right\} \psi(x, y) = 0,$$

where the magnetic field is expressed in B_0 , all lengths are measured in the magnetic length $l_B = \sqrt{\hbar c / eB_0}$, energy is measured in units of $\hbar\omega_c$, with $\omega_c = eB_0 / m_e c$ the cyclotron frequency and the velocity is expressed in units of $l_B \omega_c$. H and p_y commute due to the special form of the gauge, and consequently the wavefunction becomes

$$\psi(x, y) = \frac{1}{\sqrt{2\pi}} e^{-iky} \phi_{n,k}(x), \quad (5)$$

which reduces the problem to the solution of the 1D Schrödinger equation

$$\left[-\frac{1}{2} \frac{d^2}{dx^2} + V_k(x) \right] \phi_{n,k}(x) = E_{n,k} \phi_{n,k}(x), \quad (6)$$

where it is the k -dependent effective potential

$$V_k(x) = \frac{1}{2} [xB_z(x) - k]^2, \quad (7)$$

which contains the two dimensionality of the problem. We will solve Eq. (6) numerically by use of a discretization procedure. In some limiting cases analytical results can be obtained.

III. IN THE ABSENCE OF A BACKGROUND MAGNETIC FIELD

Let us first consider the case when no background magnetic field is present. The situation is then symmetric, and more easily to solve. The effective potential for this case is shown in Fig. 1(a) for $k = -2$ (dotted curve) and

$k = 2$ (solid curve). We notice from Eq. (7) that this potential is built from two parabolas, with minima situated at $x^l = -k$, and $x^r = k$, thus respectively on the left and right hand side of the magnetic edge. The total potential has for $k > 0$ two local minima respectively at $x = -k$ and $x = +k$, while for $k < 0$ it has only one minimum at $x = 0$. Before we describe the energy spectrum of the snake orbits and their corresponding properties, we first discuss the limiting behaviour.

A. Limiting behaviour for $k \rightarrow \pm\infty$

For $k \rightarrow \infty$, the minima of the parabolas are situated far from each other. The electrons are in the Landau states of two opposite magnetic fields, one on the left, the other on the right, and they are not interacting with each other. The electron wavefunctions are given by $\langle L|x \rangle = C_m H_m(x+k)e^{-(x+k)^2/2}$, and $\langle R|x \rangle = C_m H_m(x-k)e^{-(x-k)^2/2}$, respectively, where $H_m(x)$ is the Hermite polynomial. For decreasing k the parabolas shift towards each other, and the electrons will start to “feel” each other. In terms of wavefunctions, this results in a parabolic cylinder function $\phi(x) = D_{E-\frac{1}{2}}[\sqrt{2}(x-k)]$ matched at $x = 0$, with the condition that $\frac{d}{d\alpha} D_{E-\frac{1}{2}}(\alpha)|_{\alpha=-\sqrt{2}k} = 0$ or $D_{E-\frac{1}{2}}(-\sqrt{2}k) = 0$, for the symmetric and the antisymmetric wavefunction, respectively. This leads to a change in energy of the electron states, which can be understood as a lifting of the degeneracy of the two original electron wavefunctions. The energy can then be written as $E_{\pm}(k) = \langle L|H|L \rangle(k) \pm \langle L|H|R \rangle(k) = E(k) \pm \Delta E(k)$ with the corresponding wavefunctions $|\phi \rangle = |R \rangle \mp |L \rangle$. One can see that the presence of the second parabola results in two effects: (1) a decrease of $E(k)$ due to the finite presence of the wave function in the other parabola, and (2) a splitting of the energy level due to the overlap, i.e. one level (E_+) shifts upwards, while the other (E_-) shifts down. For $k \rightarrow \infty$, this results in the following first-order approximation to E and ΔE :

$$E_m(k) = \frac{1}{2} + m - \frac{2^{m-1}}{m! \sqrt{\pi}} k^{2m-1} e^{-k^2}, \quad (8a)$$

$$\Delta E_m(k) = \frac{2^m}{m! \sqrt{\pi}} e^{-k^2} k^{2m+1}. \quad (8b)$$

In the other limit $k \rightarrow -\infty$, the effective potential can be approximated by a triangular well $V(x) = k^2/2 - kB_0 x$. Solutions for this potential consist of Airy functions, again matched at $x = 0$ with the condition that $\phi'(0) = 0$ or $\phi(0) = 0$ which results, respectively into the anti-symmetric wavefunction $\phi_{2m}(x) = C_{2m}(k) (|x|/x) Ai \left[z_{Ai',m+1} + (2k)^{1/3} |x| \right]$ and a symmetric one $\phi_{2m+1}(x) = C_{2m+1}(k) Ai \left[z_{Ai,m+1} + (2k)^{1/3} |x| \right]$, respectively with energy

$$E_{2m}(k \rightarrow -\infty) = \frac{1}{2} \left[k^2 - z_{Ai',m+1} (2|k|)^{2/3} \right], \quad (9a)$$

$$E_{2m+1}(k \rightarrow -\infty) = \frac{1}{2} \left[k^2 - z_{Ai,m+1} (2|k|)^{2/3} \right], \quad (9b)$$

where $z_{Ai,n}$ ($= -2.338, -4.088, -5.521, \dots, -[3\pi(4n-1)/8]^{2/3}$) and $z_{Ai',n}$ ($= -1.019, -3.248, -4.820, \dots, -[3\pi(4n-3)/8]^{2/3}$), denote respectively the n^{th} ($n = 1, 2, 3, \dots, \infty$) zero of the Airy function and of its derivative. One can see that for increasing negative k , the difference between the two energy branches increases, which is to first order linear in $|k|$. Namely the more negative k , the narrower the well, thus the more the energy levels are shifted from each other.

B. Spectrum and velocity

Solving Eq. (6) numerically gives rise to the energy spectrum shown (solid curves) in Fig. 2(a). For $k = \infty$, we obtain the earlier mentioned Landau levels, which are labelled with the quantum number m . Each level is twofold degenerate. For decreasing k , the degeneracy is lifted and they separate into two different branches with eigenstates $|2m\rangle$ and $|2m+1\rangle$ and eigenvalues E_{2m} and E_{2m+1} , and corresponding quantum numbers $n = 2m$ and $n = 2m+1$. This quantum number n does not only result from arranging the levels according to their lowest energy, starting with $n = 0$, but it also reflects the number of nodes of the corresponding wavefunction. Notice that the levels have now a non-zero derivative, i.e. electrons propagate in the y -direction, and their group velocity is given by $v(k) = -\partial E(k)/\partial k$. (The minus sign appears here because in Eq. (5) we took $k_y = -k$). This group velocity is plotted (solid curves) in Fig. 3(a) for the 6 lowest levels. For $k = \infty$ electrons are in a Landau level, and consequently there is no net current in the y -direction. Decreasing k , results in a net current in the y -direction, which is positive for the upper branches ($2m+1$), but is initially negative for the branches ($2m$). For more negative values of k it increases almost linearly with increasing $|k|$, which becomes the first order analytical result $v_m(k \rightarrow \infty) = -k$, obtained by differentiating (9a) and (9b).

C. Classical picture

The center of the classical orbit corresponds to a zero in the effective potential. The energy spectrum can be divided up into three regions which can be classically understood by the electron orbits drawn in Fig. 1(a). In region (A) the electrons move in closed orbits either in the magnetic field on the left or on the right hand side. Since its cyclotron radius is smaller than the distance to the magnetic field discontinuity, they feel a homogeneous magnetic field. There is no net velocity. In region (B) the

cyclotron radius intersects the magnetic field discontinuity slightly, i.e. in such a way that the moving electron and the center of its orbit are on the same side. The electron is nevertheless able to penetrate in the opposite magnetic field region, which results in a (rather small) propagation in the y direction $v_y > 0$. For $k = 0$ the center of the orbit is exactly on the edge between the two opposite magnetic fields. In region (C) the center is located in the opposite magnetic field region of which the electron is moving in, resulting in a faster propagation of the electron in the y -direction. These different regions are also indicated in Fig. 2(a).

We can also make a quantitative classical study of the velocity, starting from the quantum mechanical energy spectrum. Since in classical mechanics there is no quantization, we make use of the obtained quantum energy spectrum in order to find the classical energy and thus the radius of the cyclotron orbit. Classically, the energy is contained in the circular velocity v_φ through $E(k) = v_\varphi^2(k)/2$. For any given quantum mechanical $E(k)$ -value we obtain classically the circular velocity $v_\varphi(k) = \sqrt{2E(k)}$. Now if we consider $x_0 = \pm k$ to be the center of the electron orbit, we can calculate for every k -value the classical velocity $v_y(k)$, since we also know $v_\varphi(k)$ and the cyclotron radius $R(k) = v_\varphi(k)$. Using geometric considerations, we obtain the following relation

$$v_y(k) = v_\varphi(k) \sqrt{1 - [k/v_\varphi(k)]^2} / \arccos[k/v_\varphi(k)], \quad (10)$$

which is shown in Fig. 3(a) by the dotted curves. Comparing this with its quantum mechanical counterpart, we notice that for $k < 0$ values good agreement is found, but for $k > 0$ there is a large discrepancy. Moreover, one can see that negative velocities cannot exist classically.

The critical k -value, k^* , for which no classical propagating states can exist, i.e. the electron describes just a circular orbit in a homogeneous magnetic field, has to be equal to the cyclotron radius $k^* = R(k^*) = v_\varphi(k^*) = \pm \sqrt{2E(k^*)}$, which leads to the boundary drawn in Fig. 2(a) (dotted parabola).

IV. WITH A BACKGROUND MAGNETIC FIELD

With a background magnetic field three different configurations: a) $0 < B < B_0$, b) $B = B_0$, and c) $B_0 < B$ must be considered. In the following we will study the snake orbits in these configurations.

A. $0 < B < B_0$

Applying a background magnetic field $0 < B < B_0$, results in a situation which is very similar to the previous one. Again the two magnetic fields have opposite sign, but in this case they also have a different strength, i.e. $B^l = -B^r/p$. Again we can calculate analytically

the correction to the energy in the limit $k \rightarrow \infty$. For an electron on the right hand side in the m^{th} Landau state of a magnetic field with strength $B^r = B_0$, the deviation from the Landau energy due to the presence of the other parabola in the effective potential is given by the following matrix element, which to second-order reads

$$E_m(k \rightarrow \infty) = |\langle R | H | R \rangle (k)| \\ = \left[m + \frac{1}{2} \right] - \frac{2^{m-2}}{m! \sqrt{\pi}} \left(1 + \frac{1}{p} \right) k^{2m-1} e^{-k^2}. \quad (11)$$

For an electron on the left hand side, i.e. in the smaller magnetic field $B^l = -B_0/p$ region, in the m^{th} Landau level, this results in

$$E_m(k \rightarrow \infty) = |\langle L | H | L \rangle (k)| \\ = \frac{1}{p} \left[m + \frac{1}{2} \right] - \frac{2^{m-2}}{m! \sqrt{\pi}} \left(1 + \frac{1}{p} \right) k^{2m-1} e^{-k^2}. \quad (12)$$

Also in this case the energy is smaller than the corresponding Landau energy. The downward energy shift decreases for increasing p .

If p is an integer, Landau states on the left and right hand side, respectively with quantum number $p \cdot m$ and m , coincide for $k \rightarrow \infty$. As a consequence these states have an overlap, which reads to first order

$$\langle L | H | R \rangle = (-1)^{m+1} 2^{m(p+1)/2} \left(\frac{1}{(pm)! m! \pi} \right)^{1/2} \\ \times p^{pm/2} e^{-k^2(1+p)/2} k^{m(p+1)+1}. \quad (13)$$

One can see that for decreasing magnetic field, i.e. increasing p , this function decreases because of the exponential factor. The electron wavefunction in the lower magnetic field region is extended over a larger region, and further away from the other (center at kp). The overlap therefore decreases with increasing p . As a result of this, the energy for $k \rightarrow \infty$ and $p > 1$ is given by $\langle R | H | R \rangle$ and $\langle L | H | L \rangle$.

For $p = 1$, we obtain the previous result, but for increasing p , the second order term in Eqs. (11) and (12) becomes more important than Eq. (13), because of the exponential factor. The splitting is lifted, and the main contribution to the negative velocity for $k \rightarrow \infty$ arises from Eq. (13) due to the finite extend of the wavefunction in the other parabola.

As an example we studied numerically the case when a background magnetic field $B = B_0/2$ is applied, i.e. $B^l = -B_0/2$ and $B^r = 3B_0/2$. As one can see in Fig. 1(b), this results in two parabolas with different minima and confinement strength. The resulting spectrum (see Fig. 2(b)) is very similar to the one of the previous case, but unlike the previous symmetrical case, not all states are twofold degenerate for $k \rightarrow \infty$. We now obtain two different sets of Landau states, corresponding to electrons moving in different magnetic field regions with different strength. In this case the second Landau level on

the left coincides with the first on the right. The classical picture for the three different regions corresponds to the one drawn in Fig. 1(b), and is also similar to the previous case, except for the different cyclotron radii. With this picture in mind, one can again calculate the classical velocity, which turns out to be identical to Eq. (10). From Fig. 3(b) we notice that again we obtain good agreement for $k > 0$, but for $k < 0$, there is a large discrepancy. The negative velocity can also in this case not be explained classically.

The critical k -value $k^* = \sqrt{2E(k^*)}$ for which snake orbits are classically possible are indicated by the parabola in Fig. 2(b).

B. $B = B_0$

When a background magnetic field $B = B_0$ is applied, we obtain the magnetic barrier studied in Ref. 17, where the magnetic field is different from zero only in the region $x > 0$, i.e. $B^l = 0$ and $B^r = 2B_0$. From Fig. 1(c) one can see that in this case the potential is made up of only one parabola and on the left side it is a constant $k^2/2$. The energy spectrum and corresponding velocities for this particular case are shown in Fig. 2(c) and 3(c), respectively. We notice that for $k \rightarrow \infty$ we again obtain Landau states, which correspond to bound states on the right hand side of the magnetic edge. Consistent, as being a limiting case of the former magnetic field states, i.e. $p = \infty$, the energy decreases with decreasing k and there is no splitting of the energy levels. Thus now we only have states which propagate with negative velocity to which we cannot assign a classical interpretation.

Also in this case we can divide up the spectrum into three regions: (A) the electrons move in closed orbits in the magnetic field region on the right hand side, (B) electrons are free, propagate forward and are reflected on the barrier and (C) electrons are free, propagate backward and are reflected on the magnetic edge. Notice that for a free electron, the energy is larger than $k^2/2$, since now the electron also propagates in the x -direction and consequently has an additional kinetic energy $k_x^2/2$.

Classically, propagating states in the magnetic field region do not exist, only Landau states do. The boundary where these classical trajectories are possible is again given by $k^* = \sqrt{2E(k^*)}$.

C. $B_0 > B$

By applying a background magnetic field with strength larger than $B > B_0$, we arrive at the situation where $0 < B^l < B^r$. The magnetic fields on the left and the right hand side have the same sign, but a different strength, i.e. $B^l = B^r/p$.

To obtain the energy in the limits $k \rightarrow \pm\infty$, we again can approximate the wavefunction as being in a Landau

state in the corresponding magnetic field. We found

$$\begin{aligned}
E(k \rightarrow \infty) &= \langle R | H | R \rangle (k) \\
&= \left[m + \frac{1}{2} \right] \\
&\quad - \frac{2^{m-2}}{m! \sqrt{\pi}} \left(1 + \frac{1}{p} \right) k^{2m-1} e^{-k^2}, \quad (14)
\end{aligned}$$

for an electron on the right hand side in the m^{th} Landau state of a magnetic field with strength $B^r = B_0$. For an electron on the left hand side, in the smaller magnetic field $B^l = B_0/p$ in the m^{th} Landau level, we have

$$\begin{aligned}
E(k \rightarrow -\infty) &= \langle L | H | L \rangle (k) \\
&= \frac{1}{p} \left[m + \frac{1}{2} \right] + \frac{2^{m-2}}{m! \sqrt{\pi}} \left(1 + \frac{1}{p} \right) k^{2m-1} e^{-k^2}, \quad (15)
\end{aligned}$$

which results in a negative velocity.

The energy spectrum and the velocity of these eigenstates for the case when $B = 3B_0/2$, i.e. $B^l = B_0/2$, $B^r = 5B_0/2$, are plotted respectively in Fig. 2(d) and 3(d). The center of the orbit is situated on the right side for $k > 0$, for $k < 0$ it is on the left side. For $k \rightarrow \pm\infty$, the electrons move in a homogeneous magnetic field (on the left ($k \rightarrow -\infty$) or right ($k \rightarrow +\infty$) hand side of $x = 0$), and thus $v_y = 0$.

From Fig. 1(d) one notices that there is only one minimum in the effective potential because the minima of both parabolas are now situated on the same side. The trajectories corresponding with regions (A), (B), and (C) are depicted in Fig. 1(d). The trajectories in region (A') are similar to those in (A) but now for a magnetic field on the left hand side, i.e. with smaller strength.

Geometrical considerations yield the following classical velocity

$$\begin{aligned}
v_y(k) &= 2v_\varphi(k) \sqrt{1 - [k/v_\varphi(k)]^2} \\
&\quad \times \{ B^l \arccos[-k/v_\varphi(k)] \\
&\quad + B^r \arccos[k/v_\varphi(k)] \}^{-1}, \quad (16)
\end{aligned}$$

which is plotted in Fig. 3(d) as dotted curves together with the quantum mechanical group velocity. One can see that, in contrast to the previous cases, the negative velocity can be understood as classical snake orbits, but these snake orbits all run in the same y -direction and now there are no states with $v_y > 0$.

Notice that the quantum mechanical velocity exhibits a small oscillatory behaviour on top of a uniform profile. These whiggles can be understood from the electron distribution over the two parabolas (see Fig. 4). With increasing k , the electron distribution is shifted from the left parabola to the right one. Due to the wavelike character of this distribution, the probability for an electron to be in the right parabola (integrated solid region in the inset of Fig. 4) exhibits whiggles as function of k , with n maxima as shown in Fig. 4. Energetically it is

favourable for an electron state to have as much as possible electron probability in the lower potential region. Consequently, when the electron probability in the lower potential region attains a maximum, a maximum downward energy shift will be introduced on top of the overall energy change, and this will result in a maximum in the group velocity.

V. NEGATIVE VELOCITY STATE

Formally, the existence of the quantum mechanical negative velocity state can be attributed to the fact that shifting two one dimensional potential wells towards each other results in a significant rearrangement of the energy levels in the composite potential well. Because the composed well is broader, some states, p.e. the ground state, have an energy which is lower than in each of the individual narrower wells. In this particular case, the wave vector k measures the distance of the two wells to each other, and consequently this energy decrease results in a negative group velocity $-\partial E/\partial k$. In this section we focus on these negative group velocity states.

Since the negative velocity states are present for any background magnetic field B , but can only be understood classically in the situation $B > B_0$, we will investigate the group velocity for a fixed k value with varying background magnetic field. In Fig. 5 the spectrum is plotted as function of the applied background field B . We have chosen $k = 1.5$ because in this case a large negative velocity is obtained for the lowest level when $B = 0$. Notice that for $B < B_0$: (1) almost all levels decrease in energy with increasing background field; (2) there is an anti-crossing for $E/E_0 = 0.4 + 0.458B/B_0$ (dotted line). This anti-crossing occurs when $B/B_0 = n/(n+1)$, with n the Landau level index. For this condition some of the Landau levels are degenerate in the limit $k \rightarrow \infty$ (see Fig. 2(b) for the case $n = 0$); and (3) for $B \rightarrow B_0$ the separation between the levels decreases to zero and a continuous spectrum is obtained with a separate discrete level at the anti-crossing line. The continuous spectrum for $B = B_0$ results from the scattered states in the potential of Fig. 2(c), while the discrete state is the bound state in this potential. For the considered k -value, i.e. $k = 1.5$, only one bound state is found for $B = B_0$.

The corresponding group velocity $v_y = -\partial E/\partial k$ is shown in Fig. 6. Notice that the maximum negative velocity is obtained near the anti-crossings in the energy spectrum (Fig. 5). Near $B/B_0 = n/(n+1)$ the splitting in the energy spectrum (see Fig. 2) is largest and as a consequence one of the levels is pushed strongly down in energy and consequently v_y becomes strongly negative. Notice that: (1) every level has some B/B_0 region at which $v_y < 0$, and (2) for $B/B_0 \rightarrow 1$ the velocity $v_y \rightarrow 0$, while (3) the envelope of $(v_y)_{\min}$ in Fig. 6 reaches for B/B_0 the $v_y < 0$ value of the $B = B_0$ state. For $B > B_0$ we have $v_y < 0$ for all states.

Using expressions (10) and (16), we can also calculate the classical velocity corresponding to the energy spectrum in Fig. 5. This is shown in Fig. 7. We notice that for $B/B_0 < 1$, the classical velocity has a similar behaviour as the quantum mechanical one, except for the anti-crossings and the lack of negative velocities, which do not have a classical analogon. These negative velocities appear suddenly for $B/B_0 > 1$ and exhibit more or less the same behaviour.

As was already apparent from the above study a necessary condition for the existence of the non-classical edge states is the presence of two local minima in the effective potential. In the limiting case $B = B_0$ the second minima is the limiting case of a flat region in $V_k(x)$ for $x < 0$. But not all these states have a negative velocity. How can we classify them?

From Fig. 2(a,b) one notices that initially (for rather small B values) the parabola $E = k^2/2$ separates the region where only states with positive group velocity exist, from the region where also negative velocity states are present. This is due to the fact that the value of this parabola equals the barrier height between the two parabolic wells for the corresponding k -value. When the energy exceeds this barrier, the shape of the wavefunction is not determined anymore by the separate parabolas, but by the overall composite well width. For decreasing k the well is squeezed, and thus all the energy levels are pushed upwards, resulting in a positive group velocity. Although this is not an exact rule which cannot be extended rigorously throughout the $B < B_0$ regime, it nevertheless provides insight into the k -values (or B values) for which these negative velocities states arise.

Inspection of the wavefunctions shows that there is a feature which marks the negative velocity states, and which relates indirectly to the presence of the different potential wells. It turns out that if the wavefunction or its first derivative exhibits a dip at some x which satisfies $\phi(x)\phi''(x) > 0$ and $\phi'(x) = 0$, or $\phi'(x)\phi'''(x) > 0$ and $\phi''(x) = 0$ and the condition that $\phi(x) \neq 0$, then the state has a non-classical negative velocity. This is true for every k value, as long as $B < B_0$. This is illustrated in Fig. 8 where we plot the wavefunction for $k = 1.5$, $n = 2$, with background magnetic field $B/B_0 = 0.68$ and 0.73 . The above dip in the wavefunction or its derivative (indicated by the dashed circle in Fig. 8) is a result of the different potential wells, which have their separate influence on the shape of the wavefunction, and therefore hamper the matching. The difference in $\phi(x)$ being zero (or not), can be interpreted as a generalization of matching the individual states in an asymmetric (symmetric way) when the Landau states are degenerate at $k \rightarrow \infty$.

VI. TIME DEPENDENT CLASSICAL INTERPRETATION

One can make different attempts to link a classical picture to quantum mechanics. Often the comparison starts

with a schematic classical picture which is then supported by comparing the quantum mechanical probability density with the classical one, obtained through calculation of the classical electron trajectory solving Newtons equation. For a 1D problem one can also verify the classical motion by inspection of the velocity parallel to the edge.^{13,16,19,1} For a cylindrical symmetric problem, the classical electron motion can be inferred from the magnetic moment or the circular current distribution of the electron state.⁹⁻¹² In this paper, a quantitative comparison was made by use of a quantum mechanical velocity parallel to the 1D magnetic field discontinuity. In the following, we will try a different approach where we will construct time dependent states, and in doing so we will introduce another feature, i.e. the oscillation frequency perpendicular to the magnetic edge.

A. $B = 0$

We already mentioned before that the solutions for this kind of problem are the parabolic cylinder functions $\phi(x) = D_{E-\frac{1}{2}}[\sqrt{2}(x-k)]$, matched in such a way that we have symmetric and anti-symmetric wavefunctions as is shown for $k = 2$ in Fig. 1(a). At $k = \infty$, these symmetric and antisymmetric states are twofold degenerate (see the two wavefunctions corresponding to the solid square in Fig. 1(a)). Due to this degeneracy any linear combination of these states is also an eigenstate. If we take the following linear combination

$$\begin{aligned} |m_+\rangle &= \frac{1}{\sqrt{2}} (|2m\rangle + |2m+1\rangle), \\ |m_-\rangle &= \frac{1}{\sqrt{2}} (|2m\rangle - |2m+1\rangle), \end{aligned} \quad (17)$$

we arrive at the well known Landau states, i.e. wavefunctions of electrons located in two different homogeneous magnetic field profiles. One electron is moving clockwise, while the other is moving counterclockwise. For decreasing k this degeneracy is lifted. Although taking linear combinations of states with a different energy yields a time dependent solution, we will extrapolate this picture towards all the other states. We choose a new orthonormal but time dependent basis:

$$\begin{aligned} |m_+\rangle &= (e^{iE_{2m}t}|2m\rangle + e^{iE_{2m+1}t}|2m+1\rangle) / \sqrt{2} \\ |m_-\rangle &= (e^{iE_{2m}t}|2m\rangle - e^{iE_{2m+1}t}|2m+1\rangle) / \sqrt{2} \end{aligned} \quad (18)$$

with $E_{m_+} = E_{m_-} = (E_{2m} + E_{2m+1})/2$. The resulting energy spectrum is shown in Fig. 2(a) by the dashed curves. The corresponding velocities are plotted in Fig. 9(a). For every branch there are two states $|m_+\rangle$ and $|m_-\rangle$.

With these new quantum states much better agreement is obtained with the corresponding classical results (dotted curves in Fig. 9(a)). Because of the addition of the two eigenstates the negative velocity almost disappeared. Only the lowering of the energy, as was mentioned in the limiting case (i.e. $k \rightarrow \infty$), results in a small

negative velocity, which can't be understood even in this picture. Also the boundary which indicates when classical states propagate is in much better agreement now.

Since we now have time dependent states, we can calculate a new feature: the oscillation frequency ω_x in the x -direction. The time dependent probability densities of the $|m_+\rangle$ and $|m_-\rangle$ states have the following form:

$$\begin{aligned} |\langle m_+|x\rangle(t)|^2 &= \frac{1}{2}(|\langle 2m|x\rangle|^2 + |\langle 2m+1|x\rangle|^2 \\ &\quad + 2\cos[\omega_x t] \langle 2m|x\rangle \langle 2m+1|x\rangle), \\ &= |\langle m_-|x\rangle(t + \pi/\omega_x)|^2, \end{aligned} \quad (19)$$

where $\omega_{x,m} = (E_{2m+1} - E_{2m})/\hbar$ is the quantum mechanical oscillator frequency in the x -direction.

Classically we can calculate this frequency ω_x again, using simple geometrical considerations, which results in

$$\omega_x(k) = \frac{\pi}{2 \arccos(-k/v_\varphi(k))}. \quad (20)$$

Both results are plotted in Fig. 9(b), and we obtain reasonably good agreement between the quantum (solid curves) and classical (dotted curves) results. Notice that for $|k| > k^*$, classically $\omega_x = 0$, which means that the electron does not oscillate between the two different magnetic field regions (i.e. it is not a snake orbit state), but it oscillates in a homogeneous magnetic field and consequently we obtain the time independent eigenstates corresponding to the Landau levels.

Of course this approach is only useful if proper linear combinations are possible. Unfortunately this is not the case when a background magnetic field $B \leq B_0$ is applied.

B. $B > B_0$

The above approach is also fruitful in the case when $0 < B^l < B^r$. We can again add adjacent levels, two by two, similar as described before. We can repeat exactly as was done before, and we arrive again at the time dependent states of Eq. (18). The energy spectrum of these states when $B = 3B_0/2$ is shown in Fig. 2(d), by dashed curves. From Fig. 10(a), we notice that the classical velocity is in better agreement then before, since the amplitude of the whiggles is lowered, due to the summation. The quantum mechanical oscillation frequency in the x -direction is again given by $\omega_{x,m} = (E_{2m+1} - E_{2m})$ and plotted in Fig. 10(b). We notice that since there are no degenerate states, we always have oscillating electrons. For $k \rightarrow \infty$ the electron oscillates with frequency $\omega_x = 2.5\omega_c$, while for $k \rightarrow -\infty$ the electron oscillates with frequency $\omega_x = 0.5\omega_c$, i.e. the electrons circle around in their separate homogeneous magnetic fields. This can also be seen from the classical oscillation frequency in the x -direction, which is given by

$$\omega_x(k) = \pi \left[\frac{\arccos(k/v_\varphi(k))}{B^l} + \frac{\arccos(-k/v_\varphi(k))}{B^r} \right]^{-1}. \quad (21)$$

Notice that also here whiggles in v_y are present (see Fig. 10(b)) which are not present in the classical results. It is clear that proper linear combinations can always be made, as long as $B > B_0$.

VII. CONCLUSIONS

We studied the electron states near discontinuities in the magnetic field. Different 1D magnetic field profiles, i.e. steps, were considered. The quantum mechanical energy spectrum was obtained and the group velocity of the states was calculated. Their corresponding classical orbits were found and the propagating states which are located at the magnetic field discontinuity correspond to snake orbits. Quantum mechanical magnetic edge states were found which move along the magnetic field step in opposite direction to the classical snake orbits and which cannot be understood classically. We were able to construct non stationary quantum mechanical states which closely approximate the classical solution for the symmetrical case $B^l = -B^r$ and for the more general case $B^r > B^l > B_0$.

ACKNOWLEDGMENTS

This work was partially supported by the Inter-university Micro-Electronics Center (IMEC, Leuven), the Flemish Science Foundation (FWO-VI), BOF-GOA and the IUAP-IV. J.R. was supported by "het Vlaams Instituut voor de bevordering van het Wetenschappelijk & Technologisch Onderzoek in de Industrie" (IWT) and F. M. P. is a research director with the FWO-VI. We acknowledge fruitful discussions with A. Matulis, P. Vasilopoulos, S. Badalian and J. A. Tyszynski.

* Electronic mail: peeters@uia.ua.ac.be

- ¹ F. M. Peeters and J. De Boeck, in "Handbook of nanostructured materials and technology", Edited by N. S. Nalwa, Vol. 3 (Academic Press, N. Y., 1999), p. 345.
- ² C. L. Foden, M. L. Leadbeater, J. H. Burroughes, and M. Pepper, J. Phys.: Condens. Matter **6** (1994).
- ³ A. Smith, R. Taboryski, L. T. Hansen, C. B. Sørensen, P. Hedegård, and P. E. Lindelof, Phys. Rev. B **50**, 14726 (1994).
- ⁴ A. K. Geim, I. V. Grigorieva, S. V. Dubonos, J. G. S. Lok, J. C. Maan, A. E. Filippov, and F. M. Peeters, Nature (London) **390**, 259 (1997).

- ⁵ S. V. Dubonos, A. K. Geim, K. S. Novoselov, J. G. S. Lok, J. C. Maan, and M. Henini, to appear in *Physica E* **6** (2000).
- ⁶ V. Kubrak, F. Rahman, B. L. Gallagher, P. C. Main, M. Henini, C. H. Marrows, and M. A. Howson, *Appl. Phys. Lett.* **74**, 2507 (1999).
- ⁷ M. Johnson, B. R. Bennett, M. J. Yang, M. M. Miller, and B. V. Shanabrook, *Appl. Phys. Lett.* **71**, 974 (1997); F. G. Monzon, M. Johnson, and M. L. Roukes, *Appl. Phys. Lett.* **71**, 3087 (1997); J. Reijniers and F. M. Peeters, *Appl. Phys. Lett.* **73**, 357 (1998).
- ⁸ J. Reijniers, A. Matulis and F. M. Peeters, *Physica E* **6**, 759 (2000).
- ⁹ L. Solimany and B. Kramer, *Solid State Commun.* **96**, 471 (1995).
- ¹⁰ H.-S. Sim, K.-H. Ahn, K. J. Chang, G. Ihm, N. Kim, and S. J. Lee, *Phys. Rev. Lett.* **80**, 1501 (1998).
- ¹¹ J. Reijniers, F. M. Peeters, and A. Matulis, *Phys. Rev. B* **59**, 2817 (1999).
- ¹² N. Kim, G. Ihm, H.-S. Sim and K. J. Chang, *Phys. Rev. B* **60**, 8767 (1999).
- ¹³ J. E. Müller, *Phys. Rev. Lett.* **68**, 358 (1992).
- ¹⁴ F. M. Peeters and P. Vasilopoulos, *Phys. Rev. B* **47**, 1466 (1993).
- ¹⁵ I. S. Ibrahim and F. M. Peeters, *Am. J. Phys.* **63**, 171 (1995).
- ¹⁶ S. D. M. Zworschke, A. Manolescu, and R. R. Gerhardt, *Phys. Rev. B* **60**, 5536 (1999).
- ¹⁷ F. M. Peeters and A. Matulis, *Phys. Rev. B* **48**, 15166 (1993); A. Matulis, F. M. Peeters, and P. Vasilopoulos, *Phys. Rev. Lett.* **72**, 1518 (1994).
- ¹⁸ M. Calvo, *Phys. Rev. B* **48**, 2365 (1993).
- ¹⁹ B.-Y. Gu, W.-D. Sheng, X.-H. Wang, and J Wang, *Phys. Rev. B* **56**, 13 434 (1997).
- ²⁰ F. M. Peeters, J. Reijniers, S. M. Badalian, and P. Vasilopoulos, *Microelectronic engineering* **74**, 405 (1999).
- ²¹ Y. I. Man'kov, *Soviet Physics-Solid State* **14**, 62 (1972); Y. I. Balkarei and L. N. Bulaevskii, *Soviet Physics-Solid State* **14**, 2018 (1973); A.S. Rozhavsky and R. I. Shekhter, *Solid State Commun.* **12**, 603 (1973); G. G. Cabrera and L. M. Falicov, *Phys. Stat. Sol. (b)* **61**, 539 (1974); *ibid.*, *Phys. Stat. Sol. (b)* **62**, 217 (1974); L. Berger, *J. Appl. Phys.* **49**, 2156 (1978); Y. V. Zakharov and Y. I. Man'kov, *Phys. Stat. Sol. (b)* **125**, 197 (1984).

FIG. 1. The effective potential (left part of the figure) for $k = -2$ (dotted curve) and $k = 2$ (solid curve) for the different magnetic field profiles indicated at the top of Fig. 2. The wavefunctions corresponding to the states in Fig. 2, as indicated by the corresponding symbols, are also shown. Schematic representation of the classical electron trajectories (right part of the figure) corresponding to the different regions indicated in Fig. 2.

FIG. 2. The energy spectra for different magnetic field profiles (B^l, B^r) shown on top of the figure: (a) $(-1, 1)$, (b) $(-0.5, 1.5)$, (c) $(0, 2)$, (d) $(0.5, 2.5)$. The dotted curves mark the different classical regions. The dashed curves in (a) and (b) are the average energy of two adjacent levels. The symbols correspond to the electron wavefunctions plotted in Fig. 1.

FIG. 3. The group velocity in the y -direction (parallel to the edge) of the 6 lowest branches of Fig. 3. The dotted curves correspond to the velocity calculated for the classical snake orbits.

FIG. 4. The velocity for the $n = 4$ state of Fig. 3(d), and the electron probability for the electron to be in the right part of the parabola as function of k . The inset shows the effective potential and the electron probability at the local maximum $kl_B = 3.4$.

FIG. 5. The energy spectrum at $kl_B = 1.5$ for the 40 lowest states as function of the applied background field B/B_0 .

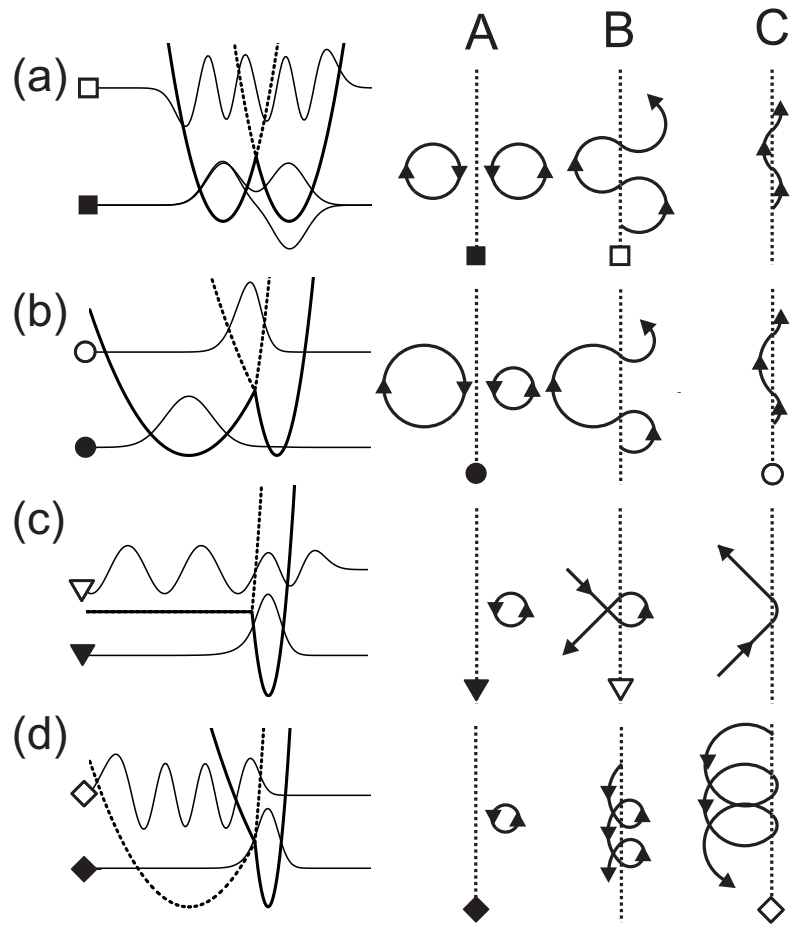
FIG. 6. The group velocity v_y as function of B/B_0 , corresponding to the electron states of Fig. 5.

FIG. 7. The classical velocity in the y -direction as function of B/B_0 , corresponding to the electron states of Fig. 5.

FIG. 8. The wavefunctions for $kl_B = 1.5$, $n = 2$ for two negative velocity states (see Fig. 6) with background magnetic field $B/B_0 = 0.68; 0.73$.

FIG. 9. (a) The quantum mechanical velocity in the y -direction (solid curves) of the time dependent states for the case $B^l = -B^r = -1$ and the velocity obtained classically (dotted curves). (b) The same as in (a) but now for the oscillation frequency in the x -direction.

FIG. 10. The same as in Fig. 9, but now for the magnetic field profile with $(B^l, B^r) = (0.5, 2.5)$.



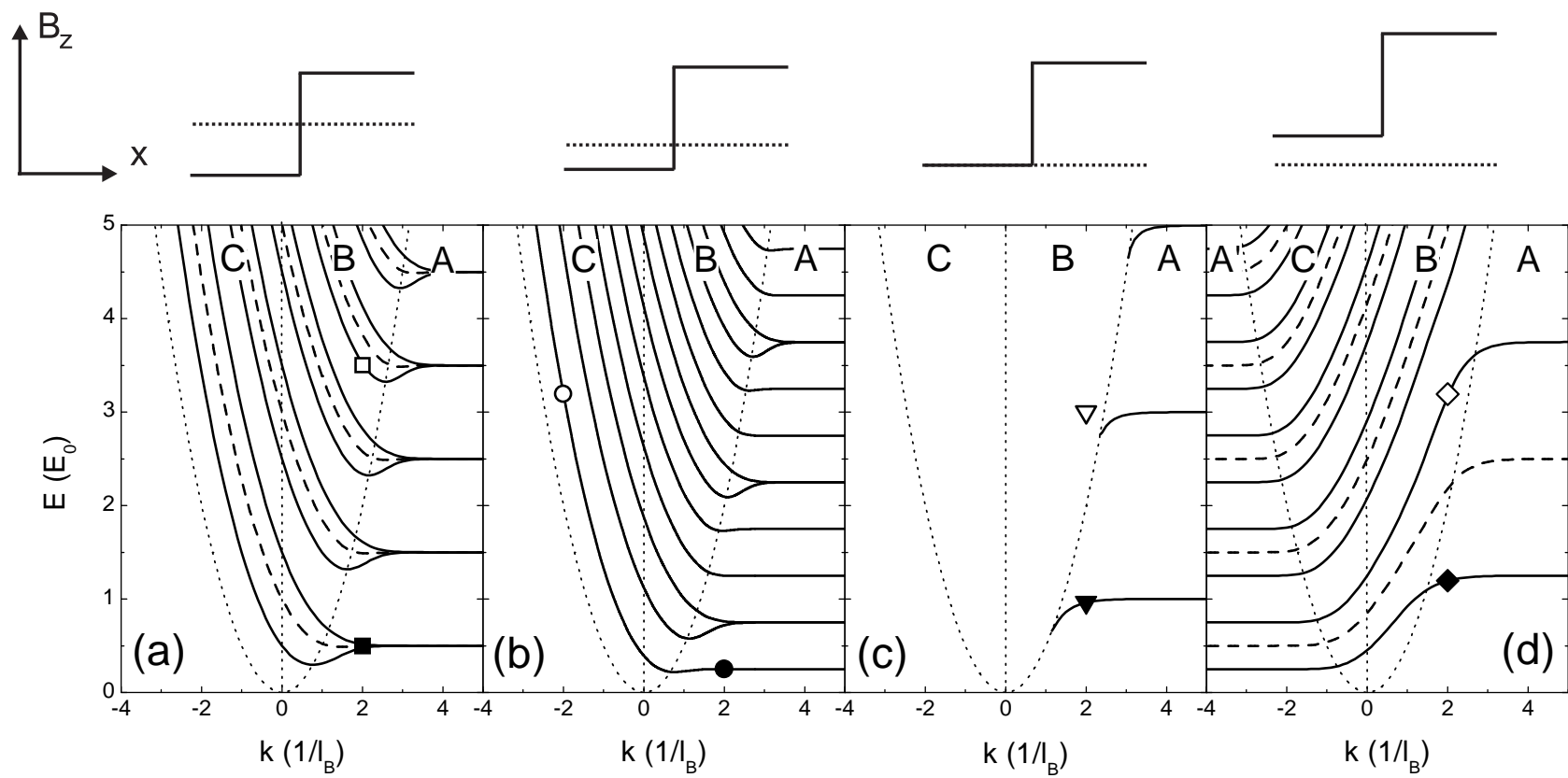
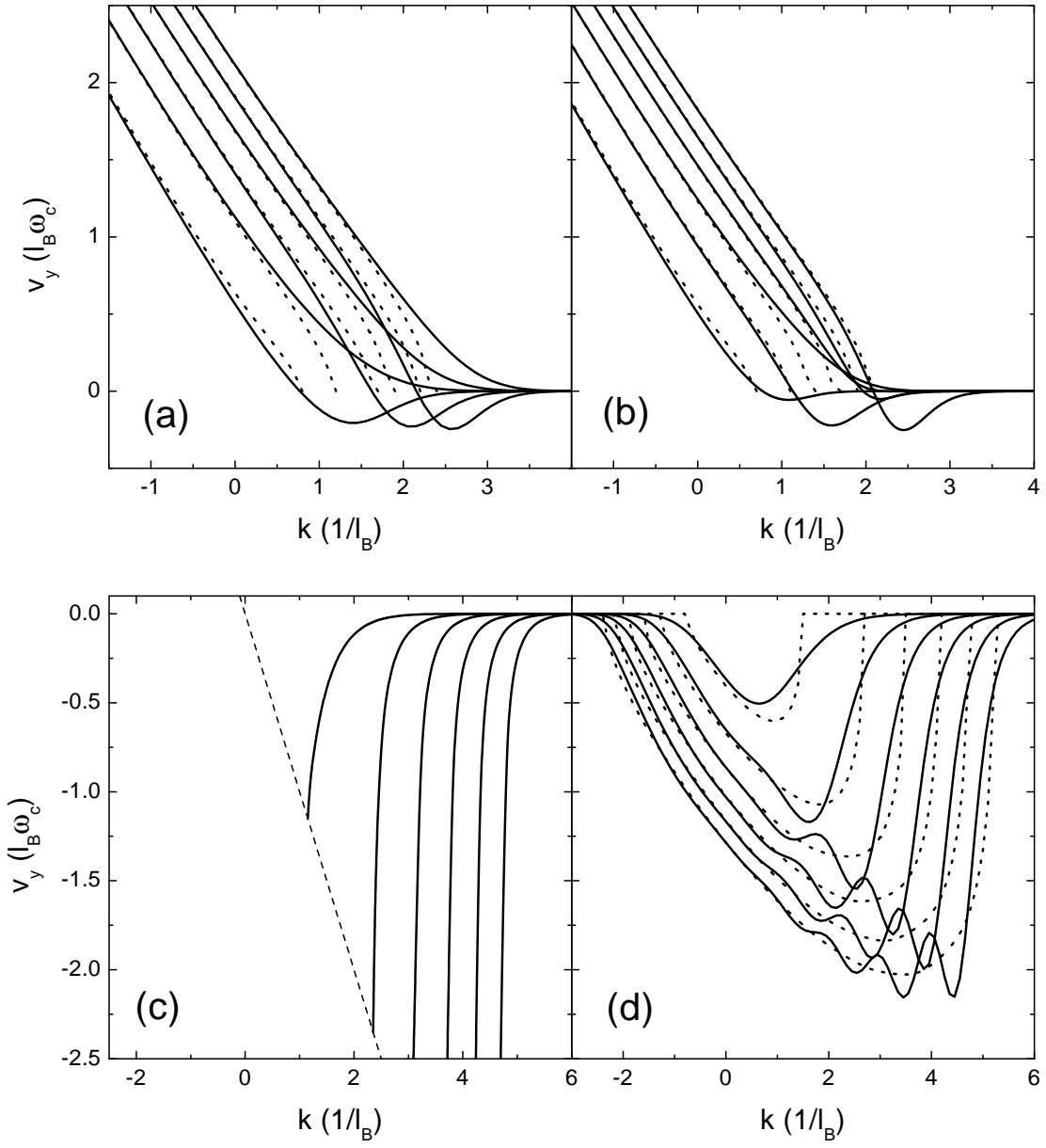


Fig. 2, Reijniers



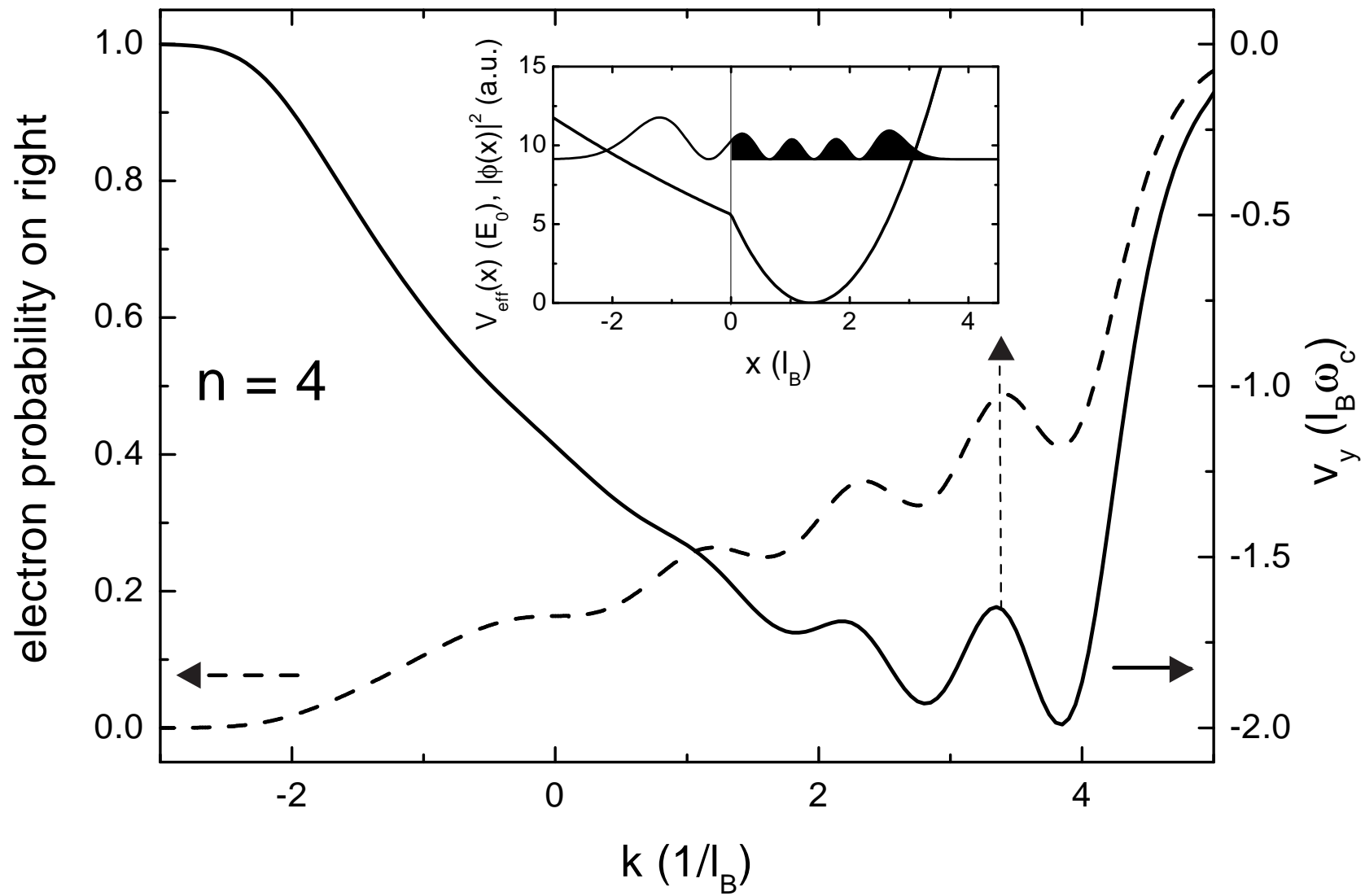


Fig. 4, Reijniers

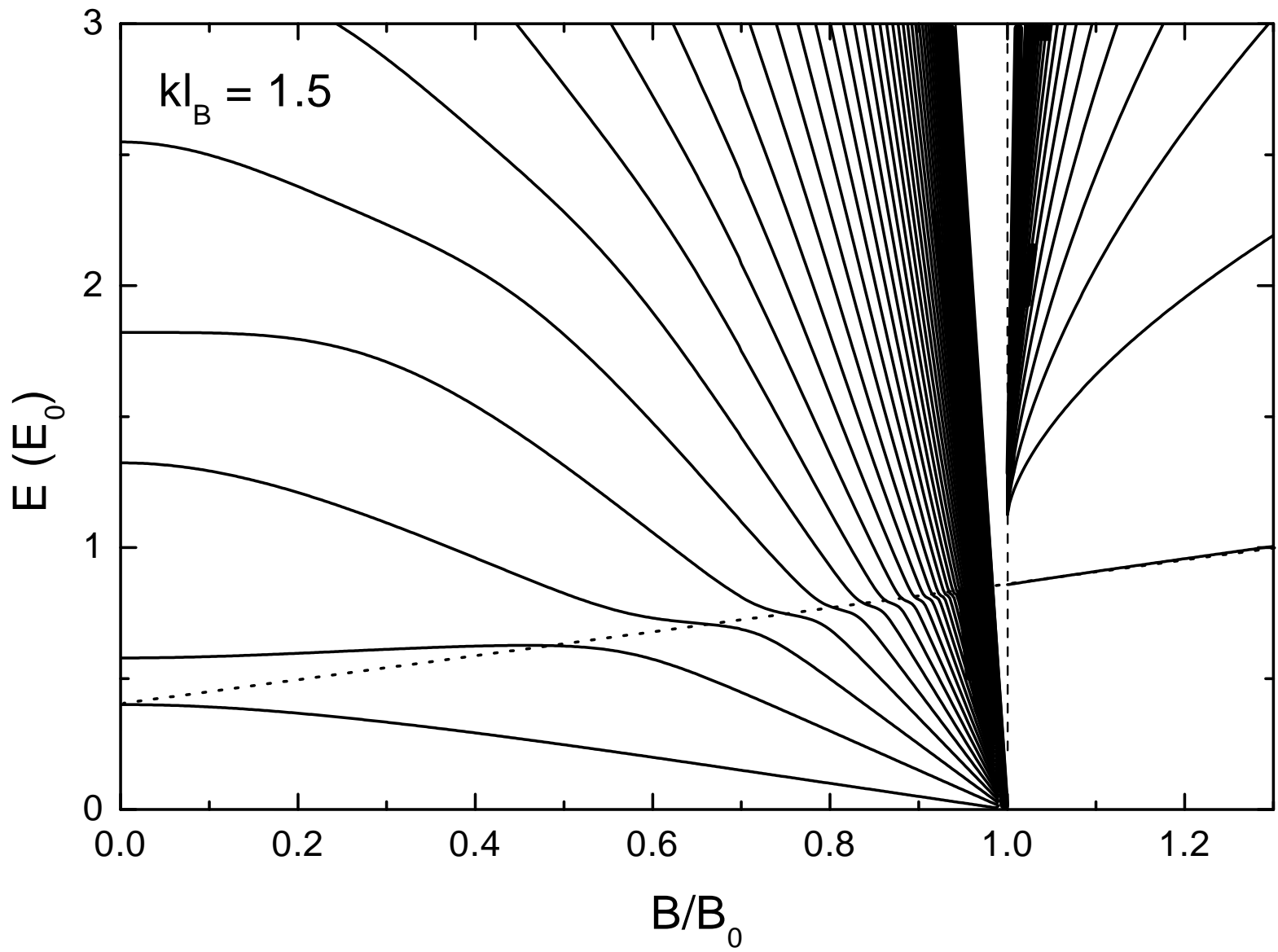


Fig. 5, Reijnders

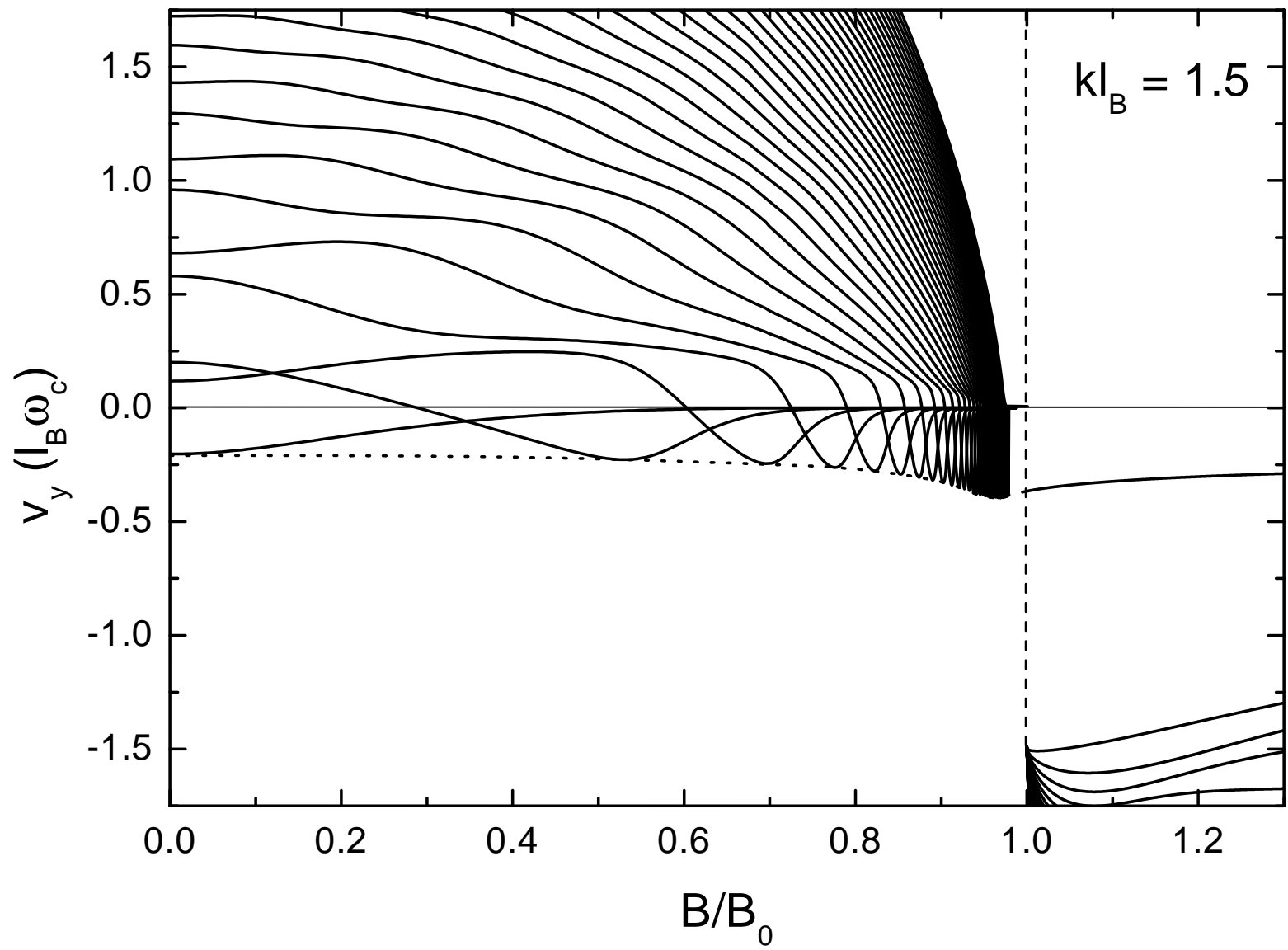


Fig. 6, Reijniers

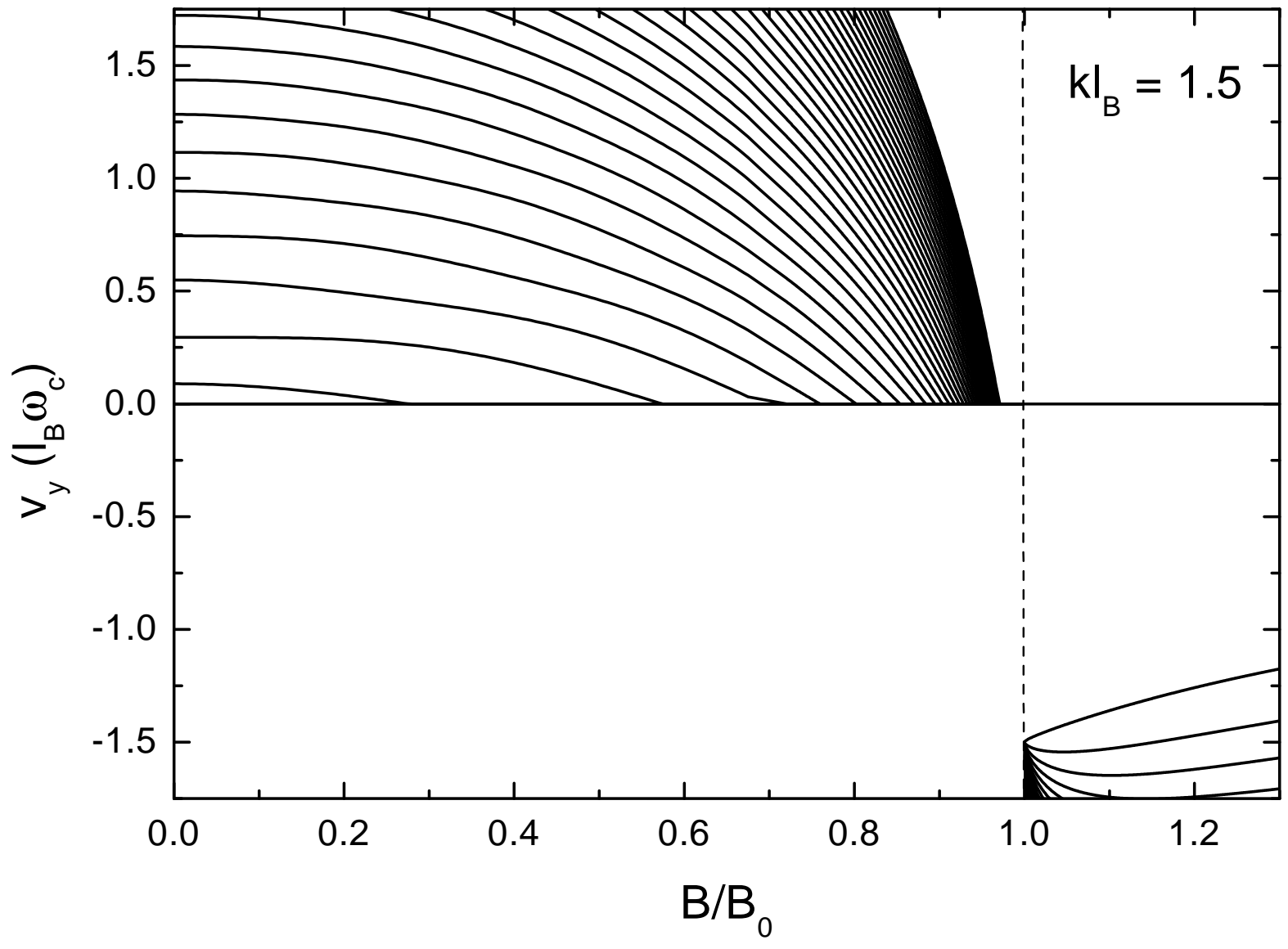


Fig. 7, Reijnders

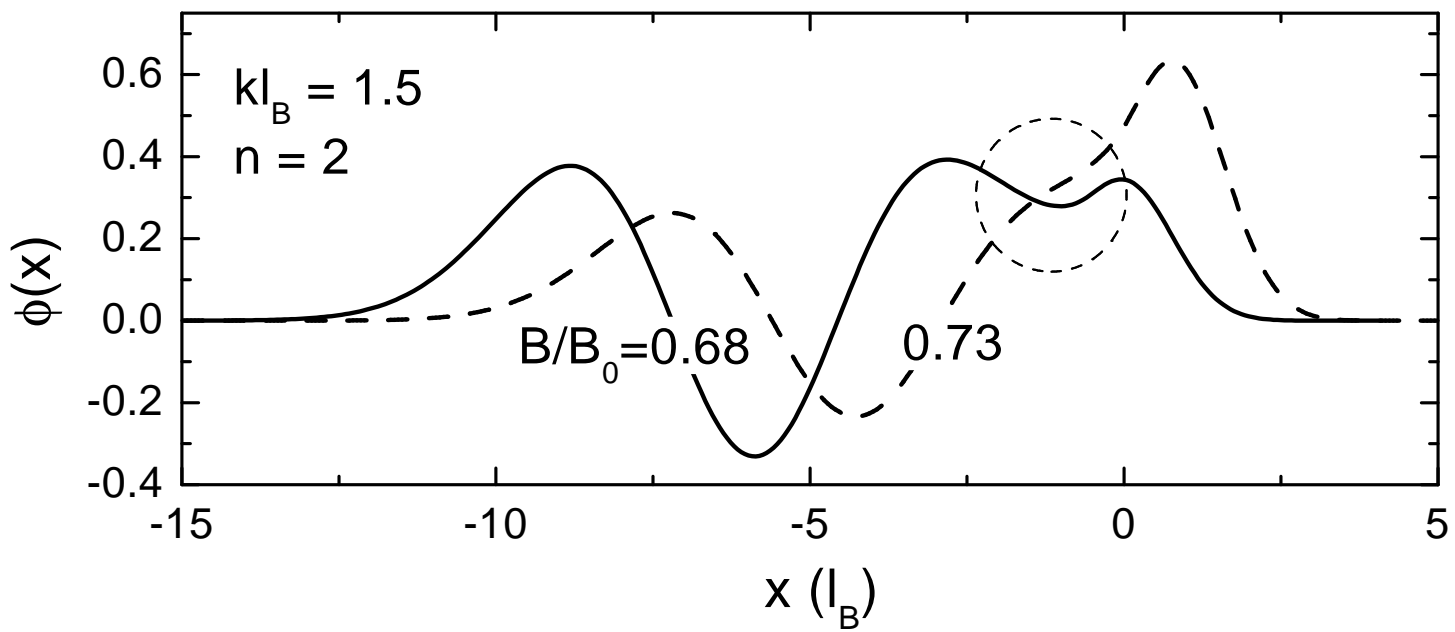


Fig. 8, Reijniers

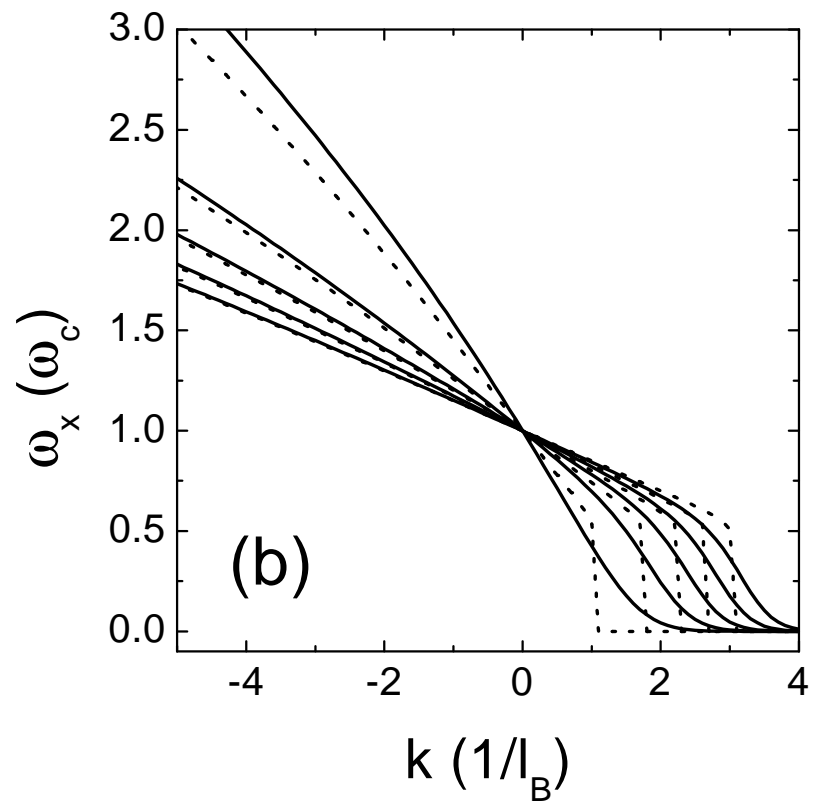
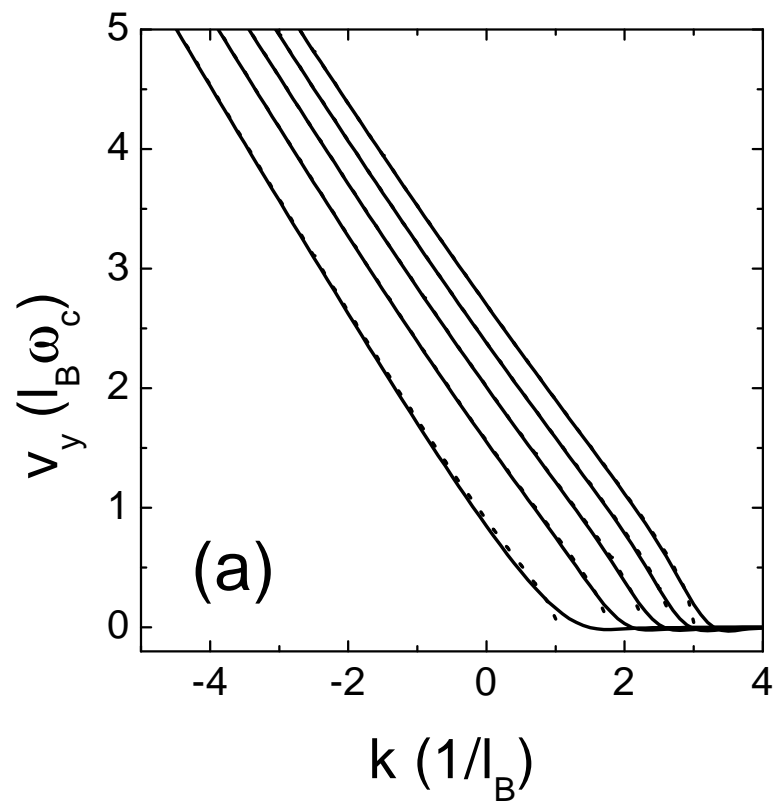


Fig. 9, Reijniers

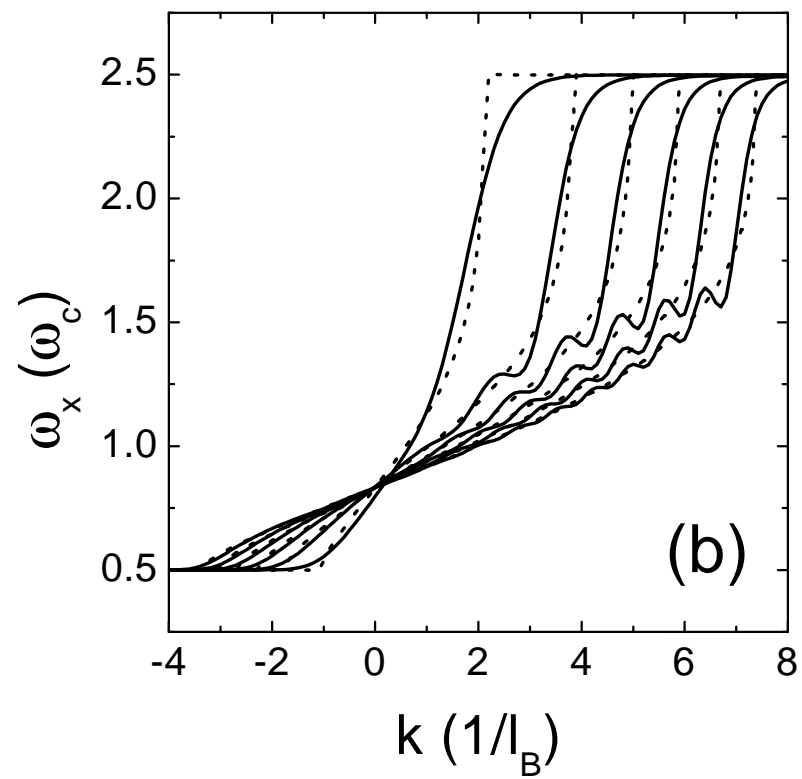
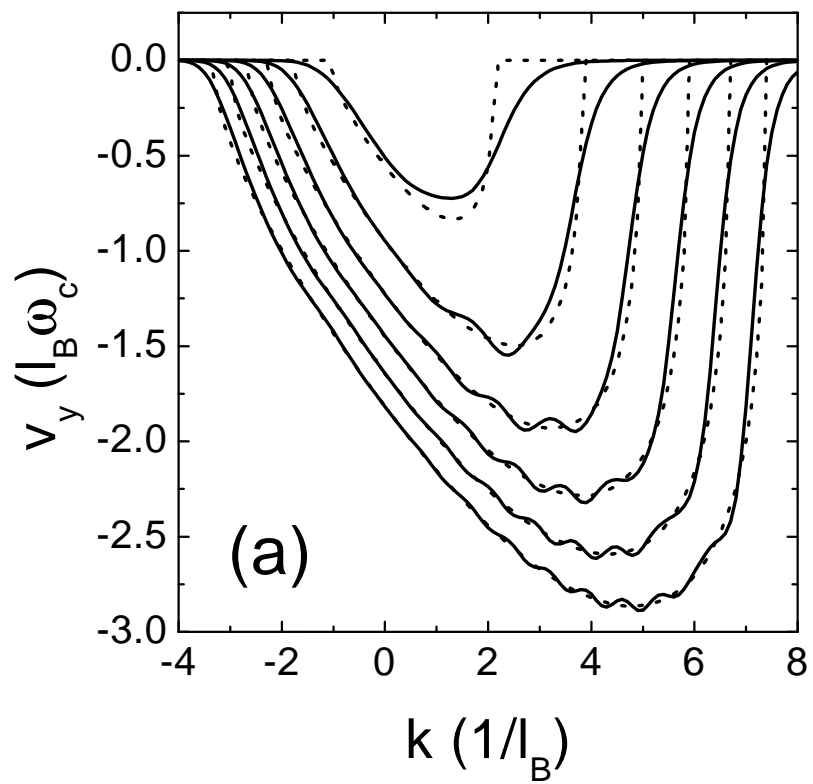


Fig. 10, Reijnders